

**SANDIA REPORT**  
SAND2004-4610  
Unlimited Release  
Printed September 2004

# **A Zero-Power Radio Receiver**

Robert W. Brocato

Prepared by  
Sandia National Laboratories  
Albuquerque, New Mexico 87185 and Livermore, California 94550

Sandia is a multiprogram laboratory operated by Sandia Corporation, A Lockheed Martin Company, for the United States Department of Energy's National Nuclear Security Administration under Contract DE-AC04-94AL85000.

Approved for public release; further dissemination unlimited.



**Sandia National Laboratories**

Issued by Sandia National Laboratories, operated for the United States Department of Energy by Sandia Corporation.

**NOTICE:** This report was prepared as an account of work sponsored by an agency of the United States Government. Neither the United States Government nor any agency thereof, nor any of their employees, nor any of their contractors, subcontractors, or their employees, makes any warranty, express or implied, or assumes any legal liability or responsibility for the accuracy, completeness, or usefulness of any information, apparatus, product, or process disclosed, or represents that its use would not infringe privately owned rights. Reference herein to any specific commercial product, process, or service by trade name, trademark, manufacturer, or otherwise, does not necessarily constitute or imply its endorsement, recommendation, or favoring by the United States Government, any agency thereof or any of their contractors or subcontractors. The views and opinions expressed herein do not necessarily state or reflect those of the United States Government, any agency thereof or any of their contractors or subcontractors.

Printed in the United States of America. This report has been reproduced directly from the best available copy.

Available to DOE and DOE contractors from  
U.S. Department of Energy  
Office of Scientific and Technical Information  
P.O. Box 62  
Oak Ridge, TN 37831

Telephone: (865) 576-8401  
Facsimile: (865) 576-5728  
E-mail: [reports@adonis.osti.gov](mailto:reports@adonis.osti.gov)  
Online ordering: <http://www.doe.gov/bridge>

Available to the public from  
U.S. Department of Commerce  
National Technical Information Service  
5285 Port Royal Rd.  
Springfield, VA 22161

Telephone: (800) 553-6847  
Facsimile: (703) 605-6900  
E-Mail: [orders@ntis.fedworld.gov](mailto:orders@ntis.fedworld.gov)  
Online ordering: <http://www.ntis.gov/ordering.htm>

## **A Zero-Power Radio Receiver LDRD 52708, FY04 Final Report**

**Robert W. Brocato  
Sandia National Laboratories  
Opto and RF Microsystems  
P.O. Box 5800  
Albuquerque, NM 87185**

***Abstract:***

*This report describes both a general methodology and some specific examples of passive radio receivers. A passive radio receiver uses no direct electrical power but makes sole use of the power available in the radio spectrum. These radio receivers are suitable as low data-rate receivers or passive alerting devices for standard, high power radio receivers. Some zero-power radio architectures exhibit significant improvements in range with the addition of very low power amplifiers or signal processing electronics. These ultra-low power radios are also discussed and compared to the purely zero-power approaches.*

**Contributors to this work include:** Gregg Wouters, Edwin Heller, Joel Wendt, Jonathan Blaich, Glenn Omdahl, Emmett Gurule, Matthew Montano, David W. Palmer, Gayle Schwartz, and Kenneth Peterson.

This page is left intentionally blank.

## **Contents**

<b>Section</b>	<b>Page</b>
Nomenclature	5
Introduction	7
SAW Correlator Overview	8
Basic Zero-Power Receiver	9
Long-code SAW Correlator Architecture	12
Signal Analysis	13
Experimental Results of Long SAW Approach	17
Zero-Power Receiver Using a Long Code Correlator	20
Conclusions	26
References	26
Distribution	27

## Nomenclature

AM	-	Amplitude modulated
ASIC	-	Application Specific Integrated Circuit
BPSK	-	Binary Phase Shift Keying
CDMA	-	Code Division Multiple Access
CMOS	-	Complementary metal oxide semiconductor
CSRL	-	Compound Semiconductor Research Laboratory
DC	-	Direct current
DS-CDMA	-	Direct Sequence Code Division Multiple Access
DSSS	-	Direct Sequence Spread Spectrum
FH	-	Frequency Hopping
FPGA	-	Field Programmable Gate Array
FY	-	Fiscal Year
GaAs	-	Gallium Arsenide
GHz	-	Giga Hertz (billion cycles/sec)
HP	-	Hewlett Packard
IC	-	Integrated circuit
IDT	-	Interdigital Transducer
IF	-	Intermediate Frequency
ISM	-	Instrumentation, Scientific, and Medical frequency band
LC	-	Inductor-capacitor circuit
LDRD	-	Lab Directed Research and Development
LNA	-	Low Noise Amplifier
MATLAB	-	Simulation software available from MathWorks
Mbps	-	Mega bits per second
MHz	-	Mega Hertz (million cycles/sec)
Mm	-	Milli-meters
OOK	-	On-Off keyed modulation
PC	-	Personal Computer
PCB	-	Printed Circuit Board
PN	-	Pseudo Noise
POP	-	Peak-Off-Peak ratio
PSAW	-	Programmable Surface Acoustic Wave correlator
PSL	-	Peak-to-SideLobe ratio (same as POP)
PSPICE	-	PC version of SPICE available commercially
RF	-	Radio Frequency
SAW	-	Surface Acoustic Wave
SNR	-	Signal to Noise Ratio
SPICE	-	Simulation Program with Integrated Circuit Emphasis
SS	-	Spread Spectrum
UWB	-	Ultra-Wide Band

## Introduction

The problem of building a radio receiver that operates without DC electrical power has been around for as long as radio has existed. Some of the earliest available radio receivers, referred to somewhat confusingly as “crystal-set” radios, used a very simple circuit with a germanium-diode detector (the “crystal”) to demodulate fairly strong AM radio stations. Early radio users did not have readily available low-cost DC power supplies or batteries and so needed to use a passive radio. Though modern users may not have the same battery constraints as in the past, they may need a radio receiver that can remain dormant for months or years. The principle behind the crystal-set radio is worth exploring, as it is the same principle that we exploit to create a modern zero-power radio receiver.

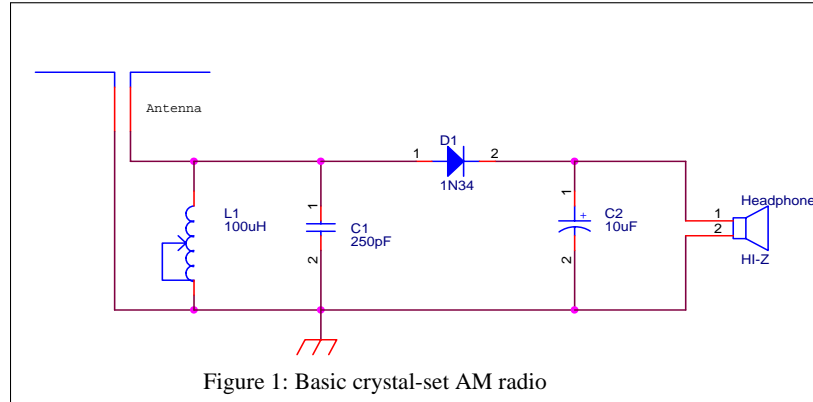


Figure 1: Basic crystal-set AM radio

The simplest crystal-set radio (figure 1) consists of an antenna, an LC-tank circuit, a diode detector, a catch capacitor, and a pair of high-impedance headphones. The antenna receives the radio waves and is tuned to the frequency band of interest. The L1-C1 circuit forms a “tank” that is an adjustable, high quality (Q) factor element that enables the receiver to tune to the particular station of interest. The Q-factor is a measure of the frequency selectivity or bandwidth of a circuit element. A high Q-factor circuit element will have a very narrow bandwidth. The 1N34 germanium diode is a demodulating detector that removes the amplitude modulation from the radio carrier frequency. The capacitor, C2, is part of the detector circuit as it works in conjunction with the diode detector to separate the modulation of the radio wave from the radio carrier wave. The high impedance headphones enable the user to hear the station information, in this case the voice or music that was originally broadcast. These basic elements of the crystal-set radio are found in any zero-power receiver and are discussed in greater detail in the following sections.

The basic principle behind both the crystal-set and other zero-power radio receivers is that they use a high-Q circuit to selectively receive a signal. They then use a demodulator to transform a very small impedance into a high impedance. The high-Q circuit selectively receives the appropriate portion of radio spectrum from the entire spectrum, and the demodulator efficiently converts a small amount of energy at a low voltage and high frequency into a slightly smaller amount of energy at a much higher voltage with a low frequency. Both of these elements are the keys to making an efficient zero power receiver. A modern zero-power receiver will include the following elements: a very high-Q circuit to select frequency, a detector to demodulate a desired signal from an RF carrier signal, and a signal processor to further refine the demodulated signal. The principles are the same as for the crystal-set radio except that the modern zero-power receiver uses a combination of approaches to increase the Q-factor of the receiver.

The special component that provides the requisite high Q-factor is the surface acoustic wave (SAW) correlator. A SAW correlator combines the narrowband, high Q-factor operation of a

bandpass filter with a coded reception scheme that further enhances Q-factor by the use of coding gain. It effectively enables the reception of a very narrow band of signals while still using a broad bandwidth to transmit the signal. The SAW correlator is a completely passive device. It uses the electromagnetic energy in the input RF wave to convert to an acoustic wave that is subsequently used in a matched filter [1]. The SAW correlator's Q-factor is directly proportional to the code length of the device. Therefore, it is important to maximize the code length of the correlator. The ideal zero-power receiver would consist of a very long SAW correlator connected directly to an antenna on one end and a highly efficient, demodulating detector on the other end. Limitations within the SAW correlator prevent this ideal scenario from being realized, as described in the following section.

### SAW Correlator Overview

The first key to the zero-power receiver is the SAW correlator. In its simplest form, a SAW device appears as two comb-like metal structures deposited on a piezoelectric crystal surface (figure 2). The first comb-like structure serves as a transducer to convert long wavelength radio waves to very short wavelength acoustic waves. For instance, a 3 GHz radio wave propagating in free space has a wavelength of 10cm, while a 3 GHz acoustic wave propagating in lithium niobate, a suitable piezoelectric material, has a wavelength of 0.000116 cm. The SAW takes advantage of this wavelength compression to perform signal processing on radio waves. The second comb-like structure in the SAW serves both as signal processing device and as a transducer to convert the acoustic waves back into an electromagnetic signal.

Although SAW devices may not be widely understood, they have been around for over 35 years. SAW filters are commonly used in many consumer electronic devices. A typical cellular phone contains several SAW filters. The worldwide production of SAW devices was estimated to consist of over 1 billion devices in 1999 [2]. SAW filters also have a long history of production and use at Sandia National Laboratories. SAW filters are used in communication electronics and sensor applications. Sandia uses SAW filters for a wide variety of sensor related products. The MicroChemLab is a Sandia chemical sensor-on-a-chip used to detect a range of different chemicals. In contrast to SAW filters, SAW correlators are not widely used in industry, although research into these devices has been conducted for over 30 years.

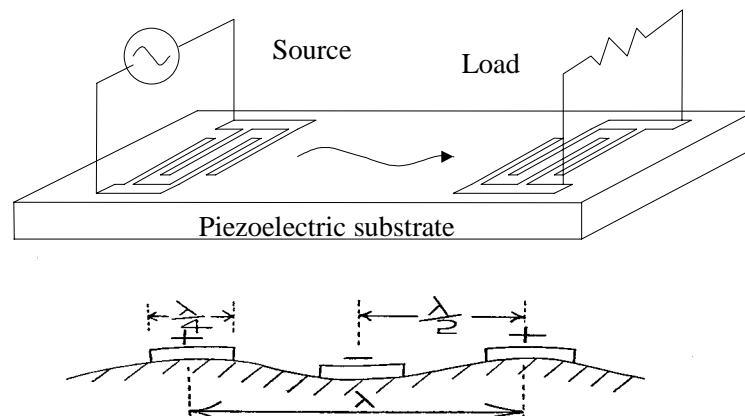
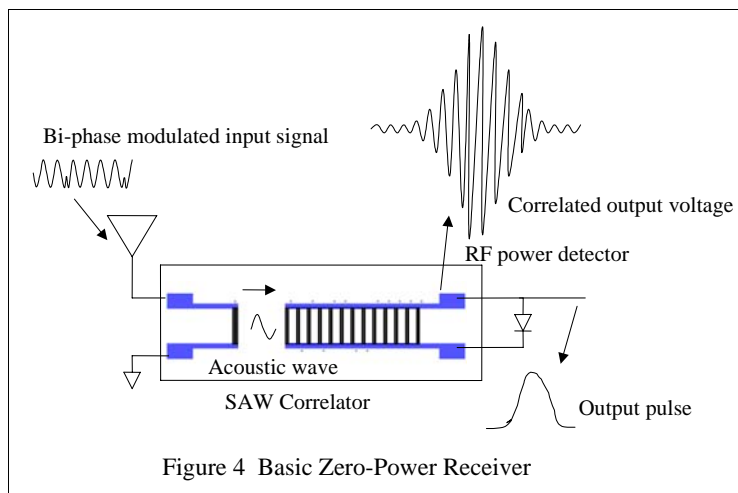
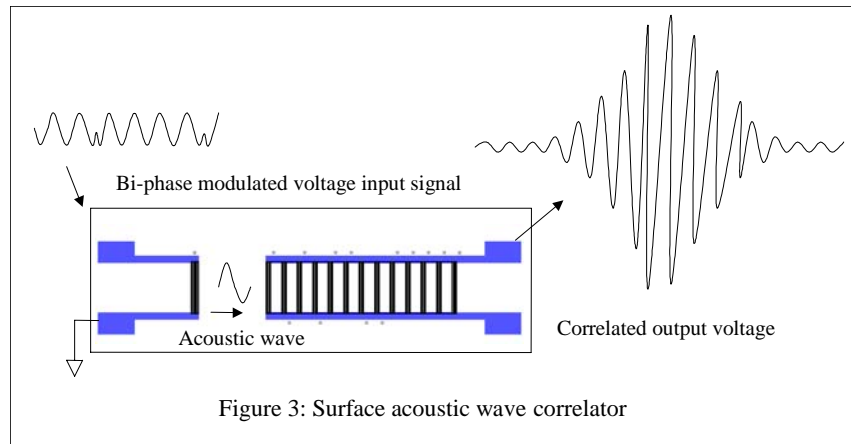


Figure 2: Surface Acoustic Wave Device



### Basic Zero-Power Receiver

A SAW correlator is a two transducer piezoelectric device used to provide a matched filter output (figure 3). The filter, in the case used here, matches to a BPSK phase modulated signal, rather than the usual sine wave. That is, the incoming radio wave has 180 degree phase transitions in its sinusoidal waveform, modulated in a coded pattern. A transducer, or IDT, in the front end of the SAW correlator converts the electromagnetic wave to a surface acoustic wave. SAW correlators use this electromagnetic to acoustic wavelength compression to perform bi-phase coded signal processing on a radio wave that has been converted into an acoustic wave. The correlator first has a transducer to convert radio waves into acoustic waves at a selected center frequency and with a selected bandwidth. The correlator then has a phase coded receiver transducer to convert the correctly phase coded acoustic wave into an RF modulated electrical pulse. Envelope detection of the modulated pulse yields a baseband electrical pulse. This pulse can be used for low data rate communications or to turn on a higher-power consumption, higher- data rate receiver. The correct correlation coded signal is essentially a long multi-bit “key”. The correlator output signals the correct “key” by outputting a voltage spike. If an incorrect code is given, the correlator output appears similar to broadband noise.

With the addition of a passive microwave detector to its output, the correlator shown in figure 3 becomes the most basic of zero-power radio receivers (figure 4). One simply needs to make a long enough correlator with a low enough insertion loss and a detector diode with a low enough

insertion loss, and one has a reasonably efficient zero-power receiver. The only drawback to the simple configuration shown in figure 4 is the insertion loss through the correlator and detector. If an application has sufficient RF power (i.e. is used at close range) or if the output is usable with a small voltage pulse, then this configuration is probably adequate. Attenuation through a typical 31-chip, 2.4GHz correlator is about 14dB (5x decrease in voltage), while attenuation through a typical optimized RF detector diode is about 20dB (10x decrease in voltage signal). Coding gain from the correlator about makes up for the attenuation through that device, but the losses through the passive detector are still significant. Building a detector that uses a tiny bias current can improve the detector from a 20dB loss to about a 6dB gain in signal. For really long-range applications, more sophisticated approaches must be used to obtain both long code correlators and low loss detectors.

Configuration of correlator circuit	Input signal level	SAW loss	Detector loss	Output voltage	Output noise (rms)	SNR
Passive 31-chip SAW with passive diode	700mVpp / +7dBm	-14dB	-27dB	7mV	<10uV	>700
	200mVpp / -6dBm	-14dB	-50dB	100uV	<10uV	>10
Passive 31-chip SAW with powered detector	700mVpp / +7dBm	-14dB	+6dB	200mV	300uV	670
	100mVpp / -10dBm	-14dB	0dB	20mV	300uV	67
	25mVpp / -22dBm	-14dB	-20dB	0.5mV	300uV	1.33

The chart shown above outlines two different approaches to a basic SAW correlator-based zero-power receiver. The first device uses a passive 31-chip SAW correlator coded with an optimal m-sequence code. The center frequency of the correlator is 2.43GHz and the bandwidth is 80MHz at the 3dB points. Each correlator chip is 30 cycles long to achieve this bandwidth. The detector is a passive MA/COM 2086-6000 microwave diode. The entire arrangement uses no DC power at all. This arrangement is not very sensitive in terms of output signal voltage for a given input power level. However, output signal-to-noise levels are very high with detector output noise levels being below the threshold of the instrument used to measure them. The output signal levels are low enough with this approach that some very sensitive means of observing the signal is necessary, but the very low noise level may still make this circuit useful for some applications. The losses shown above do not take into consideration the process gain obtained by using the correlator.

The second approach described in the chart uses the same 31-chip m-sequence SAW correlator with a 2.43GHz center frequency and 80MHz bandwidth. Instead of a passive detector, it uses a specially designed micro-powered square law detector that shifts the square law region to a much more voltage-sensitive level than the passive microwave diode. The circuit to achieve this result is discussed in a later section. This powered detector was measured at an operating voltage/current of 1.8v/400uA (720uW) for continuous operation. When operating in a pulsed mode for a wake-up circuit with a 0.1% duty cycle, its power consumption drops to 3.6uW. Detector operation is only slightly degraded from the results indicated when operated at 1.0v/100uA (100uW, continuous). When operating in a pulsed mode under these bias conditions, the total power consumption drops to 0.5uW. Power consumptions of this magnitude can typically be scavenged from surroundings. The detection threshold using this approach is reached for an input level of -22dBm. This is still a moderately high input signal strength, but is a large

improvement in sensitivity over the entirely passive approach. The detector circuit dominates the noise output of this approach.

The correlators used in this work make use solely of BPSK signals. The correlator can provide considerable process gain by converting the input BPSK signal with a matched pattern into an RF modulated pulse with an envelope at the baseband frequency. The baseband envelope pulse is then recovered using a microwave detector diode operating optimally in its square law region. A high frequency correlator can be used without IF stages by directly converting the input coded RF signal into an output baseband pulse. Figure 4 shows this basic receiver approach with the SAW correlator's output section divided into the equal phase-coded sections referred to as "chips". The modulated output pulse of such a device operating at 2.4GHz is shown in figure 6. The number of chips in the correlator determines the code length of the device. This analog conversion approach rejects multi-path and other spurious signals to the same degree as comparable DSSS systems. Furthermore, the entire system can be used in a UWB mode where the signal exists unobtrusively with the rest of the RF spectrum. It is no more difficult to build a UWB correlator than a narrowband device. The correlator can be operated in forward or reversed mode to produce low power, low component count receivers and transmitters.

A significant drawback to using this approach is the limited code length that can be achieved with conventional SAW correlators. The SAW correlator output transducer converts acoustic energy to electrical energy, typically being electrically terminated in some low impedance such as  $50\Omega$  to enable high frequency operation. Each chip section of the output transducer converts a portion of the acoustic wave that passes under it into electrical power in the real part of the output impedance. By the time the acoustic wave has passed under about 30 chip-sections of the output transducer, its amplitude has decayed so significantly, that there is little signal left with which to do further correlations. Figure 5 shows the output response of a 2.43GHz, 31 chip long SAW correlator after it has been excited with a burst of RF at the center frequency of the device and with a number of cycles equal to the number of cycles in one chip. This excitation waveform essentially forces the code of the correlator out at the center frequency of excitation. The noteworthy aspect of this figure is the rapid decay in amplitude of the output waveform from the first chips to the last. This rapid decay is a direct result of operating the high speed SAW driving into a low electrical impedance. Historically, this decay was much less significant in low frequency, high impedance devices [3]. This decay in correlator response has the same effect when operating as a receiver and severely limits the useful code length of the correlator for high-speed devices.

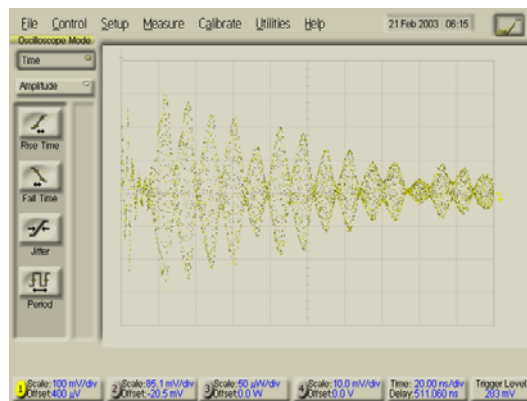


Figure 5: SAW correlator output at 2.43GHz.

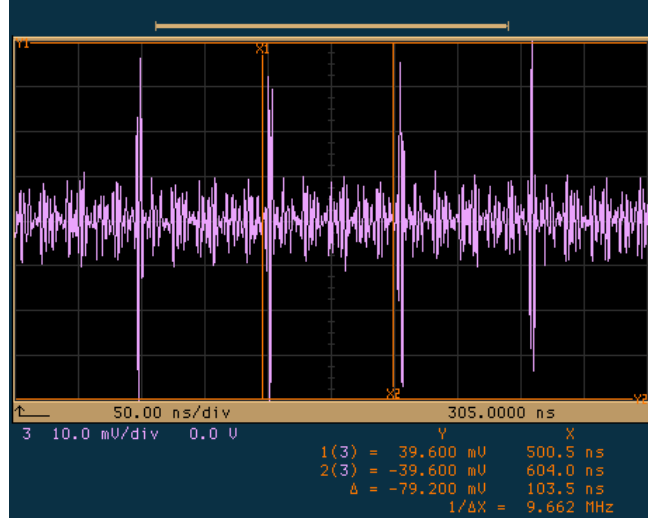


Figure 6: SAW correlator output in normal operation.

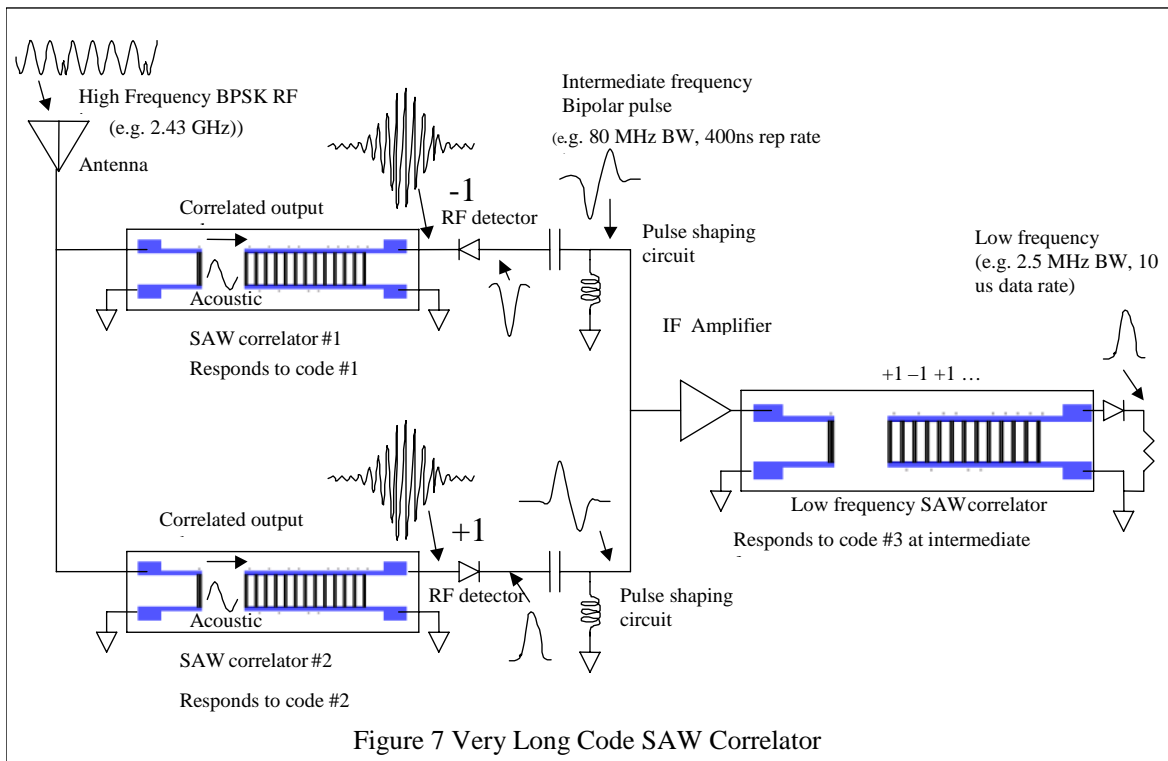
This limitation in correlator code length,  $N$ , limits the process gain available from the device, since the best possible process gain available from a correlator is equal to  $N$ . In a correlator, the process gain corresponds to the peak-to-sidelobe (PSL) ratio, which is  $N$  for a synchronously filled Barker code device. The longest Barker code only has  $N=13$ . For longer codes, such as maximal length sequence codes, the PSL is more typically  $(4N)^{1/2}$  or lower [4]. Ideally, one would like to make the process gain a very large number, but the acoustic attenuation through the device limits correlator length for a single acoustic device to about 31 chips, especially in high frequency, low impedance devices.

### Long-code SAW Correlator Architecture

The solution to building SAW correlators with arbitrarily long codes able to operate directly on GHz input signals is to split the correlation process up into sections that do not excessively attenuate the acoustic signal. Amplifiers can be used in between these sections to boost the signal level back, or impedance transformations can provide higher voltage signals with diminished power. Since each section involves a demodulation and decrease in frequency, the process is similar to a heterodyne approach, except that it does not require the use of mixers. The first correlators in such a chain operate directly at RF frequencies, while subsequent correlators that operate at lower frequencies are referred to as IF stage correlators. This architecture is shown in fig. 7. The resulting code length of this correlator is  $N1*N2$  where  $N1$  is the code length of the first pair of correlators and  $N2$  is the code length of the low frequency stage correlator.

Starting with the BPSK signal from the antenna input at the left side of the diagram, the signal passes through a power splitter and is introduced simultaneously to two orthogonally-coded SAW correlators, each operating directly at the RF carrier frequency. When the bottom correlator receives its code, it responds with an RF modulated pulse at its output. This signal is arbitrarily called the +1 code. The other correlator minimally responds to this code. The correlator output for the +1 code is then detected using a positive polarity RF detector. The resulting envelope is turned into a bipolar pulse using a passive shaping circuit. This demodulated signal is equal to the chip rate of the first two correlators and becomes the IF frequency. Concomitantly, the other input correlator responds to the signal code designated as the -1 code. Its output is detected using a negative polarity RF detector. The output of its shaping circuit is an oppositely polarized bipolar pulse, also at the IF.

The input to the third, or IF, correlator is then composed of the stream of +1 and -1 bipolar pulses that derive from the two input correlators. An amplifier can be inserted in the pulse stream after the signal is recombined from the two input correlators, but is not needed for some applications. The composite code introduced to the first two correlators must be built up to render a code sequence of +1 and -1 pulses in the code sequence and at the center frequency of the IF correlator. The output of the IF correlator is then detected using a matched Schottky diode, and the final signal is at the baseband frequency. The IF correlator operates at a much lower frequency than the input correlators. This means that its load impedance can be much higher than 50Ω, and it can be much longer than 31 chips. Its length is primarily limited by the physical size that can be accommodated on a wafer. A three-inch LiNbO<sub>3</sub> wafer will just accommodate a 63-chip correlator at 62MHz. Using such a correlator with a pair of 2.4GHz input correlators; a combined length of 1953 chips is feasible. Still longer codes are possible by using broader bandwidth input correlators, with fewer cycles per chip, and thus raising the IF frequency and shortening the length of the IF correlator for a given number of chips.



### Signal Analysis

The long code SAW correlator can be described mathematically in terms of convolution integrals of the input BPSK signal with the SAW IDTs. In order to proceed with a more detailed discussion of the resulting signals, it is first necessary to define terms, as follows:

- $t$  = time, typically in nsec for GHz simulations
- $f_{oi}$  = center frequency of the first input correlators
- $f_{oo}$  = IF or center frequency of the IF correlator
- $N_{Bi}$  = number of cycles per chip in input correlators
- $N_{Bo}$  = number of cycles per chip in IF correlator
- $N_{ci}$  = number of chips in input correlators 1 and 2
- $N_{co}$  = number of chips in IF correlator

$T_{ci} = N_{Bi} / f_{oi} =$  chip time of input correlators  
 $T_{co} = N_{Bo} / f_{oo} =$  chip time of IF correlator  
 $T_{Bi} = N_{Bi} N_{ci} / f_{oi} =$  bit time of input correlators  
 $T_{Bo} = N_{Bo} N_{co} / f_{oo} =$  bit time of IF correlator  
 $f_{ci} = 1 / T_{ci} =$  chip rate of input correlators  
 $f_{co} = 1 / T_{co} =$  chip rate of IF correlator  
 $f_{Di} = 1 / T_{Bi} =$  data rate of input correlators  
 $f_{Do} = 1 / T_{Bo} =$  data rate of complete assembly  
 $a_{x1} = 1, -1, -1, 1, 1, \dots =$  BPSK input code, corr. 1  
 $a_{x2} = -1, -1, 1, 1, -1, \dots =$  orthogonal code, corr. 2  
 $b_{x1} = 1, 1, -1, -1, 1, \dots =$  time reversed input1 code  
 $b_{x2} = -1, 1, 1, -1, -1, \dots =$  time reversed input2 code  
 $c_{jo} = 0, 0, 1, 1, 1, \dots =$  IF correlator input code  
 $d_{jo} = 1, 1, 1, 0, 0, \dots =$  time reversed IF corr. code  
 $u(t) = 0$  if  $(t < 0)$ , else  $1 =$  unit step function

The input BPSK signal (figure 8) to obtain a correct response from the first of the input correlators can be described as a stream of sine waves with varying phases as seen in

$$v_{i1}(t) := \sin(2\pi f_{oi} t) \cdot \sum_{x=1}^{N_{ci}} a_{x1} \left[ u \left[ t - (x-1) \cdot T_{ci} \right] - u \left( t - x T_{ci} \right) \right]$$

The BPSK input signal to the second of the input correlators uses a code that is orthogonal to the code of the first input correlator. The input BPSK signal to obtain a correlation output pulse from this correlator is

$$v_{i2}(t) := \sin(2\pi f_{oi} t) \cdot \sum_{x=1}^{N_{ci}} a_{x2} \left[ u \left[ t - (x-1) \cdot T_{ci} \right] - u \left( t - x T_{ci} \right) \right]$$

Here  $a_{x1}$  and  $a_{x2}$  are the coefficient vectors that are mutually orthogonal. Both of these input signals consist of a sine wave at the center frequency of the input correlator modulated by the chip sequence of the input codes. Each will excite a single correlation pulse output from one of the input correlators. The correlator output transducer serves as a matched filter to the input BPSK signal. The impulse response of the transducer for the first correlator is

$$c_{i1}(t) := \sin(2\pi f_{oi} t) \cdot \sum_{x=1}^{N_{ci}} b_{x1} \left[ u \left[ t - (x-1) \cdot T_{ci} \right] - u \left( t - x T_{ci} \right) \right]$$

The electrical input signals  $v_{i1}(t)$  and  $v_{i2}(t)$  must pass through input transducers to be converted into acoustic waves. This input transducer typically consists of  $N_{Bi}$  finger-pairs of metal spaced at the center frequency of the correlator. The impulse response of this type of input transducer for the first correlator is given by

$$p_{i1}(t) := \sin(2\pi f_{oi} t) \cdot (u(t) - u(t - T_{ci}))$$

and typically  $p_{i1}(t) = p_{i2}(t)$ . These input transducers each describe a windowing function. The operation of electrically exciting this transducer with the input wave  $v_{i1}(t)$  or  $v_{i2}(t)$  is represented by a time domain convolution operation, so that the output acoustic wave is given by

$$ac_1(t) := \int_0^t v_{i1}(\tau) \cdot p_{i1}(t - \tau) d\tau$$

The acoustic wave represented by  $ac_1(t)$  (figure 9) shows some distortion due to the band limiting action of the input transducer. The wave,  $ac_1(t)$ , is then convolved with the output transducer impulse response to produce the final electrical output  $y_{o1}(t)$  of the SAW correlator. The electrical output of this convolution operation is given by

$$y_{o1}(t) := \int_0^t c_{i1}(\tau) \cdot ac_1(t - \tau) d\tau$$

This resulting output signal is a correlation pulse modulating a sinusoidal center frequency signal. Simulation results for a 31-chip input correlator at the 2.4GHz center frequency are shown in figure 10. This analysis includes the effect of the correlator input transducer, which causes some distortion to the acoustic wave (fig. 9) and, as a result, also to the output waveform (fig. 10). The second input correlator produces a corresponding  $y_{o2}(t)$  output signal by a similar convolution when excited by the  $v_{i2}(t)$  input signal.

Each of these output pulses represented by  $y_{o1}(t)$  and  $y_{o2}(t)$  must be converted into a single cycle input to the IF correlator. The correct input waveform to the complete correlator assembly is then a coded stream of the  $v_{i1}(t)$  and  $v_{i2}(t)$  signals. Each of these output pulses is first envelope detected by a microwave diode detector. This device typically operates in some combination of linear and square-law operation, depending on the strength of the input signal. The detector output is given as

$$y_{oD}(t) := k_1 \cdot (y_{o1}(t))^2 + k_2 \cdot y_{o1}(t)$$

with  $k_1$  and  $k_2$  being constants that vary with the input signal amplitude. This raw detector output (figure 11) is typically not an observed signal, as the output is further filtered by a combination of parasitic and added capacitance at the output of the detector. This filtered output signal (figure 12) is given by

$$y_{oF}(t) := \int_0^t y_{oD}(\tau) \cdot e^{-\frac{(t-\tau)}{\tau_o}} d\tau$$

The time-constant,  $\tau_o$ , of this output filter is determined by the detector video resistance  $R_v$  and the output capacitance  $C_v$ .

The output  $y_{oF}(t)$  of the diode detector is a unipolar pulse. This must be converted into a bipolar pulse to most effectively drive the input transducer of the IF correlator. Another passive circuit, a two-pole differentiator-shaping filter, easily performs this conversion process. This circuit consists of a damped LC high-pass filter with a time constant well below the input pulse bandwidth. The operation of the filtered detector output passing through this filter (fig. 13) is yet another convolution and is given by

$$y_{oB}(t) := \int_0^t \mathbf{y}_{oF}(\tau) \cdot \sin\left(\frac{t-\tau}{\tau_{o2}}\right) \cdot e^{\frac{-(t-\tau)}{\tau_{o3}}} d\tau$$

This output signal,  $y_{oB}(t)$ , represents only one bipolar pulse in a train of pulses that make up the input to the IF correlator. The input signals applied to the two input correlators must consist of a coded set of shorter length codes,  $v_{i1}(t)$  and  $v_{i2}(t)$ . The coding applied to the stream of  $v_{i1}(t)$  and  $v_{i2}(t)$  signals is itself the code,  $c_{jo}$ , of the IF correlator. The complete input waveform to generate the combined signal is

$$v_i(t) := \sum_{j=1}^{N_{co}} \left[ c_{jo} \cdot v_{i1}(t) + (1 - c_{jo}) \cdot v_{i2}(t) \right]$$

This complete BPSK input signal is  $N_{ci}N_{co}$  chips long. It is the signal that gets transmitted to the receiver and comes in at the antenna. The resulting output signal combined from the two input correlators is the sum of the two final signals,  $y_{oaB}(t)$  and  $y_{obB}(t)$ , where the subscript 'a' represents the '1' correlator and the subscript 'b' represents the '-1' correlator. Both of these signals are approximately of the form

$$y_{oa4}(t) := \sin\left(2 \cdot \pi \cdot f_{oo} \cdot t\right) \cdot \left(u(t) - u\left(t - \frac{1}{f_{oo}}\right)\right)$$

This is just a single cycle of a sine wave at the center frequency of the IF correlator. The input to the IF correlator is then a coded stream of these signals as represented by

$$v_{iIF}(t) := \sum_{j=1}^{N_{co}} \left[ c_{jo} \cdot y_{oa4}(t - j \cdot T_{co}) + (1 - c_{jo}) \cdot y_{ob4}(t - j \cdot T_{co}) \right]$$

This input signal is then transformed into an acoustic signal in the IF correlator by the input transducer. This input transducer to the IF correlator has an impulse response given by

$$p_{iIF}(t) := \sin\left(2 \cdot \pi \cdot f_{oo} \cdot t\right) \cdot \left(u(t) - u(t - T_{co})\right)$$

This is similar in form to the impulse response given by  $p_{i1}(t)$ , but the input frequency,  $f_{oo}$ , and the chip width,  $T_{co}$ , of the IF correlator are markedly different from that of the input correlators. The acoustic signal in the IF correlator is then given by

$$ac_{iIF}(t) := \int_0^t v_{iIF}(\tau) \cdot p_{iIF}(t - \tau) d\tau$$

which is the time-domain convolution of the input signal with the wideband transducer impulse response. This signal is similar in appearance to that shown in figure 9. This acoustic signal must then match the output transducer's finger pattern given by

$$c_{oIF}(t) := \sin\left(2 \cdot \pi \cdot f_{oo} \cdot t\right) \cdot \sum_{j=0}^{N_{co}-1} d_{jo} \cdot \left[u(t - j \cdot T_{co}) - u(t - (j+1) \cdot T_{co})\right]$$

The acoustic signal will be convolved with this output transducer pattern, producing an electrical signal, as given by

$$y_{oIF}(t) := \int_0^t c_{oIF}(\tau) \cdot ac_{IF}(t - \tau) d\tau$$

This signal passes through a detector diode, which has different optimization parameters from the input detector diodes. This detected signal is given by

$$y_{oIF2}(t) := k_3 \cdot (y_{oIF}(t))^2 + k_4 \cdot y_{oIF}(t)$$

Where  $k_3$  and  $k_4$  are square-law and linear region constants determined by the magnitude of the input signal  $y_{oIF}(t)$ . This raw detector output is filtered by the output capacitance of the detector circuit. This filtering process is given by

$$y_{oIF3}(t) := \int_0^t y_{oIF2}(\tau) \cdot e^{\frac{-(t-\tau)}{\tau_{oIF}}} d\tau$$

For optimum response, the time constant  $\tau_{oIF}$  is needs to be much longer than the time constant,  $\tau_o$ , applied to the input detectors. This is because the output data time,  $f_{Do}$ , to which the detector time constant should be matched, is much longer than the data time of the input correlators given by  $f_{Di}$ . This implies that the output impedance that the final detector sees can be made higher than the output impedance of the IF correlator. This provides an opportunity to increase the output signal voltage, even though power has been lost through the correlation process. This final output signal,  $y_{oIF3}(t)$ , is the output of the entire combined correlator. It is similar in shape to fig. 12 with a time constant determined by the output data time,  $f_{Do}$ . Figures 8-13 are simulated output results obtained by applying the analysis just provided with actual component values inserted for the various constants.

### Experimental Results of Long SAW Approach

A complete long SAW correlator was built using this methodology. The two input correlators operate at 2.43GHz center frequency and have orthogonal codes 31 chips long. Each chip contains 30 cycles, giving the correlator a 3.3% input bandwidth. The detector diodes are matched to about 100Ω at their input and matched to about 400Ω at their output. This is roughly an optimum match to the input SAW device, and the increase in impedance through the detector allows for an increase in signal voltage. The use of passive detectors causes significant attenuation through the entire chain. The pulse bandwidth out of the diode detectors is 80 MHz. A signal out of one of the detectors is shown in figure 14. The central peak is the correlation peak and indicates the correct detection of a signal. The sidelobes occur from minor correlations and defects in the correlation process and constitute noise through the remainder of the circuit.

The pulse shaping circuit is a two-pole differentiator with a self-resonant frequency of 8MHz. The differentiator is just a two pole LC circuit configured as a high pass filter with its corner frequency somewhat below the frequency of the input unipolar pulse. This circuit turns the unipolar pulses into bipolar pulses with a center frequency of 62MHz. A signal out of one of the shaping circuits is shown in figure 15. Because the signal is a single cycle of a sinusoid, it has a very wide bandwidth.

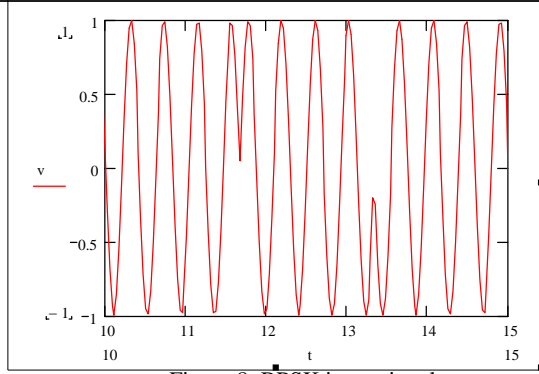


Figure 8: BPSK input signal

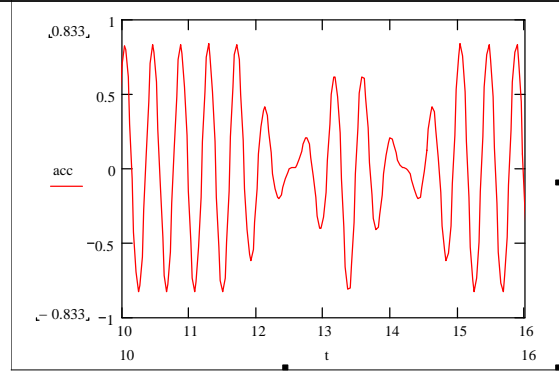


Figure 9: Acoustic signal after input IDT

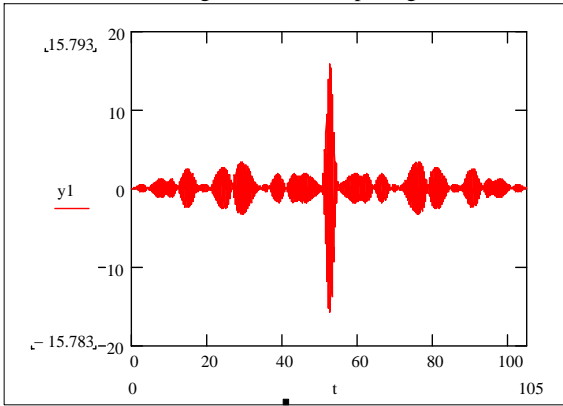


Figure 10: Correlator electrical output

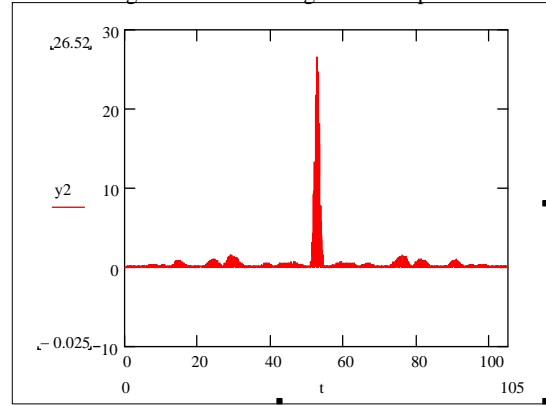


Figure 11: Raw detector output

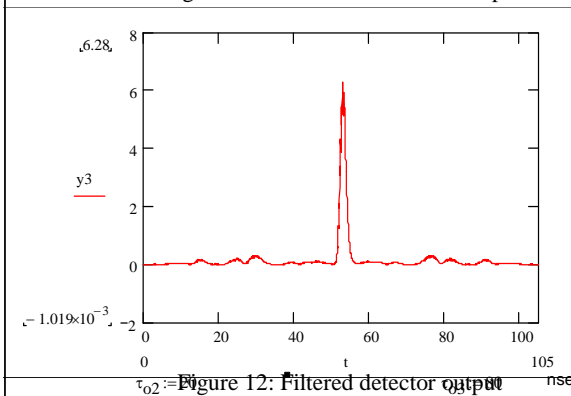


Figure 12: Filtered detector output

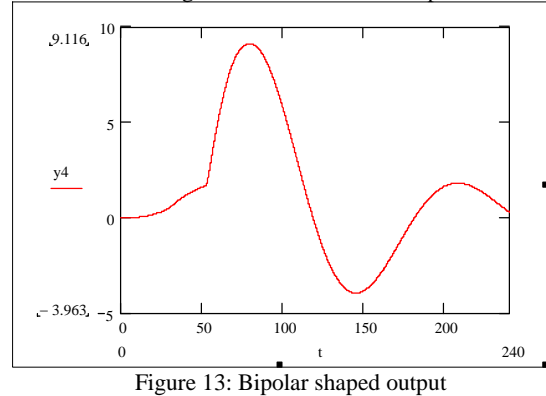


Figure 13: Bipolar shaped output

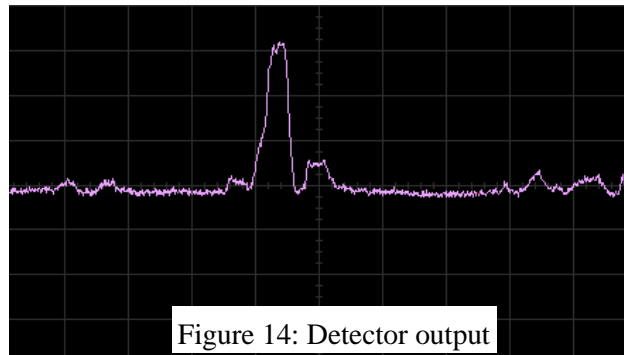


Figure 14: Detector output

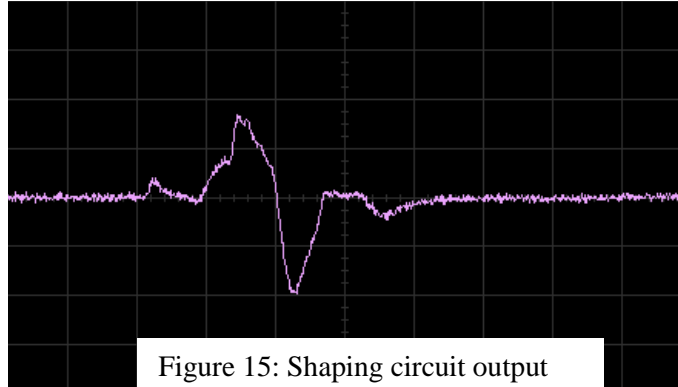


Figure 15: Shaping circuit output

The signal strength has been attenuated somewhat after passing through the correlators and the detection and shaping circuitry. For an input signal of +7dBm, the output pulse amplitude,  $y_{o4}(t)$ , after the shaping circuits is typically about 20mV peak-to-peak. The  $-1$  and  $+1$  signal lines are then combined using a Wilkinson coupler and the signal is boosted using an IF amplifier. The IF amplifier requires a gain of 20dB and a bandwidth of 100MHz. If an active detector drawing about 0.5mW is used in place of the passive detector, no IF amplifier is typically needed. The output of the IF amplifier is coupled into the IF correlator.

The IF correlator is a low frequency device, having a center frequency of 62MHz, and a bandwidth of 3.6MHz. This device is physically much larger than the input correlators, and its code length is limited by practical limitations of fabrication. A 13-chip device with 17 cycles/chip was used. This device is almost 2cm long when fabricated on YZ-cut lithium niobate, which has a velocity of 3488m/s. The output of the IF correlator before passing through its detector is shown in figure 16.

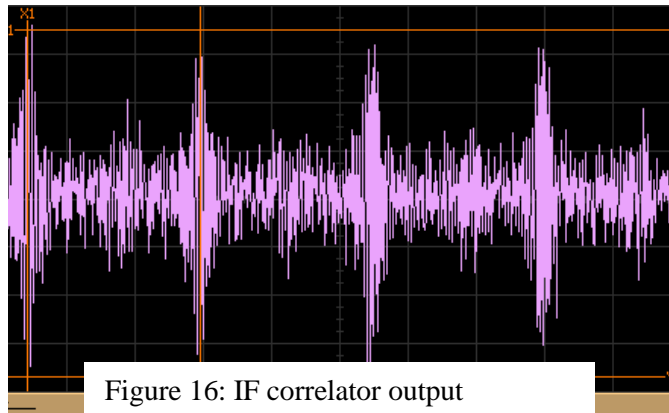
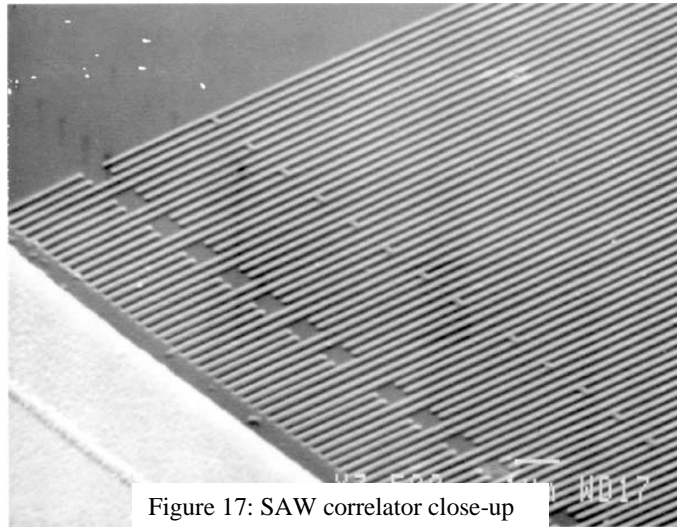


Figure 16: IF correlator output

The output of the IF correlator is processed with an RF detector, as with the input correlators. The bandwidth of the detected signal is about 200kHz, so the detector bandwidth is decreased to accommodate this low output frequency. The complete circuit has an output peak voltage of 50mV into a 100k $\Omega$ -termination impedance for a total input power of 0dBm. This only represents one possible implementation of the long SAW correlator approach. Detectors and correlators can be further optimized to enable elimination of the IF gain stage and improvement in output sensitivity. The next section covers a wide range of different implementation approaches using this architecture.

### Zero-Power Receiver Using a Long Code Correlator

The long code correlator provides a significant improvement in coding gain when used with high frequency input signals. We built a variety of different versions of this type of correlator. The all SAW correlator-based approaches use a pair of 31-chip SAW correlators in the input and a 13-chip SAW correlator at the back. The input correlators use an optimal m-sequence code, have a center frequency of 2.43GHz, and a bandwidth of 80MHz. The IF correlator uses a 13-chip Barker code, has a center frequency of 62MHz, and a bandwidth of 3.6MHz. It uses 24 cycles for each chip in the receiver. All correlators are built from lithium niobate and use 500Å of aluminum for the finger patterning and 2µm of gold for the bus bars and contact pads. A photo of one of the 2.43GHz correlators is shown in figure 17. The code length of the combined long code correlator is 403 chips. It requires 290,160 cycles of signal at 2.43GHz coded with 403 phase transitions in the correct locations with the correct phases. The correlator very strongly rejects any signal that is not at exactly the correct frequency and with exactly the correct input code.



A variety of different long SAW correlator configurations were built and tested. These do not exhaust all possibilities but reasonably cover the different options of implementing this technology. These different approaches are compared in the table shown on the next page.

The first configuration is an entirely passive SAW device. It uses three passive SAW correlator detectors. The two input SAW correlators use orthogonal m-sequence codes and are otherwise as described above. Several different passive detectors were used to demodulate the signal from the two input correlators. The performance of these different passive detectors was found to be roughly similar. The optimum passive detector for small input signals with the fast, 80MHz envelope was found to be the HSMS2852 voltage-doubler diode. One can see from the table that losses in the overall circuit are dominated by the detector losses. Due to an impedance transformation from input to output, it is possible to obtain a power loss but a voltage gain through the detector. So, very big improvements in the overall performance of the entirely passive long SAW are possible. Unfortunately, the requisite detector improvements were beyond the time and resources available to this effort. After the first passive detector, the IF correlator somewhat reduces the signal, but the final detector greatly reduces the output signal. The overall detector losses render the output signal too low to be useful as a waking device. Current demodulating detectors are designed to work with signals in the 10's to 100's of millivolts. If the input signal is very small, the detector greatly reduces the signal. This is the opposite of the desired effect. It is possible to improve passive detector performance

enough so that small input signals receive much less attenuation. In that case, an entirely passive long SAW based receiver for wake-up applications would be feasible. Designing a passive detector to enable this will require a significant future effort.

Configuration of correlator circuit	Input signal level	Input SAW	First detector	IF SAW	Output Detector	Output Signal	Pulsed DC Power
Passive 31-chip SAW, passive det., passive 13-chip SAW, passive det.	+7dBm	-14dB	-27dB	-12dB	-40dB	20uV	0uW
Passive 31-chip SAW, passive det., passive 13-chip SAW, powered det.	+7dBm	-14dB	-27dB	-12dB	0dB	1.7mW	3.5uW
Passive 31-chip SAW, powered det., passive 13-chip SAW, passive det.	+7dBm -10dBm	-14dB	+12dB 0dB	-12dB	-20dB -40dB	14mV 50uV	7uW
Passive 31-chip SAW, powered det., passive 13-chip SAW, powered det.	+7dBm -10dBm	-14dB	+12dB 0dB	-12dB	+10dB -3dB	500mV 3mV	10.5uW
Passive 31-chip SAW, powered det. w/ IF amp, passive 13-chip SAW, powered detector	-10dBm -20dBm -30dBm	-14dB	+23dB +20dB +23dB	-12dB	+12dB +3dB -3dB	500mV 35mV 4mV	40.5uW
Passive 31-chip SAW, powered det. w/ 46dB IF amp, passive 13-chip SAW, powered det., baseband amp	-30dBm -40dBm -50dBm	-14dB	+34dB +30dB +20dB	-12dB	+66dB +60dB +50dB	320mV 320mV 140mV	58.5uW
Passive 31-chip SAW, powered det. w/ IF amp, powered low freq. digital correlator circuit.	-10dBm -20dBm -30dBm	-14dB	+23dB +20dB +14dB	+20dB +30dB +40dB	na na na	3.3v 3.3v 3.3v	60uW

The other approaches use powered detectors and amplifiers in different configurations to eliminate or mitigate the severe detector losses. The second and third approaches use a very low power detector to demodulate the signal at the output of the IF correlator and at the output of the input correlators, respectively. Neither approach produces a large output signal for the +7dBm input level, though the use of a powered detector significantly increases the output level. This detector resembles a linear, common emitter amplifier, but operates as a non-linear demodulating detector (figure 18). It provides gain for small input signals, though it still significantly attenuates microvolt level signals. It operates over a wide range of supply voltages, but was characterized at a continuous power consumption of 1.8v/ 400uA. Performance is only slightly reduced at 1.0v/ 100uA. Tests were conducted to duty cycle both the detector and several amplifiers at a 1:1000 ratio. That is, when used in a wake-up function, power consumption can be greatly reduced by turning the device off and on at regular intervals. When the on-to-off ratio is kept at 1:1000, total power consumption is reduced by about 200x. These are the pulsed DC power values that are shown in the table. A typical button-cell battery's internal dissipation while sitting on a shelf ranges from about 3uW to 30uW, depending on the storage temperature. Any power consumption that is near or within this range implies that battery lifetime will be nearly equal to the shelf life of that battery. All of the powered circuits considered in this section have duty-cycled power consumption that is near to this level.

The fourth approach uses a powered detector in place of both passive detectors. The SAW correlators are all passive in this approach, and no other powered components are used. This approach produces a large, saturated output signal for the +7dBm input signal. Output signal voltage drops to a barely usable 3mV at -10dBm. This large change in output signal for a modest change in input signal is due to the nonlinearity inherent in the detector. Both powered and passive detectors exhibit significant nonlinearities, and insertion loss increases significantly at very low input signal levels.

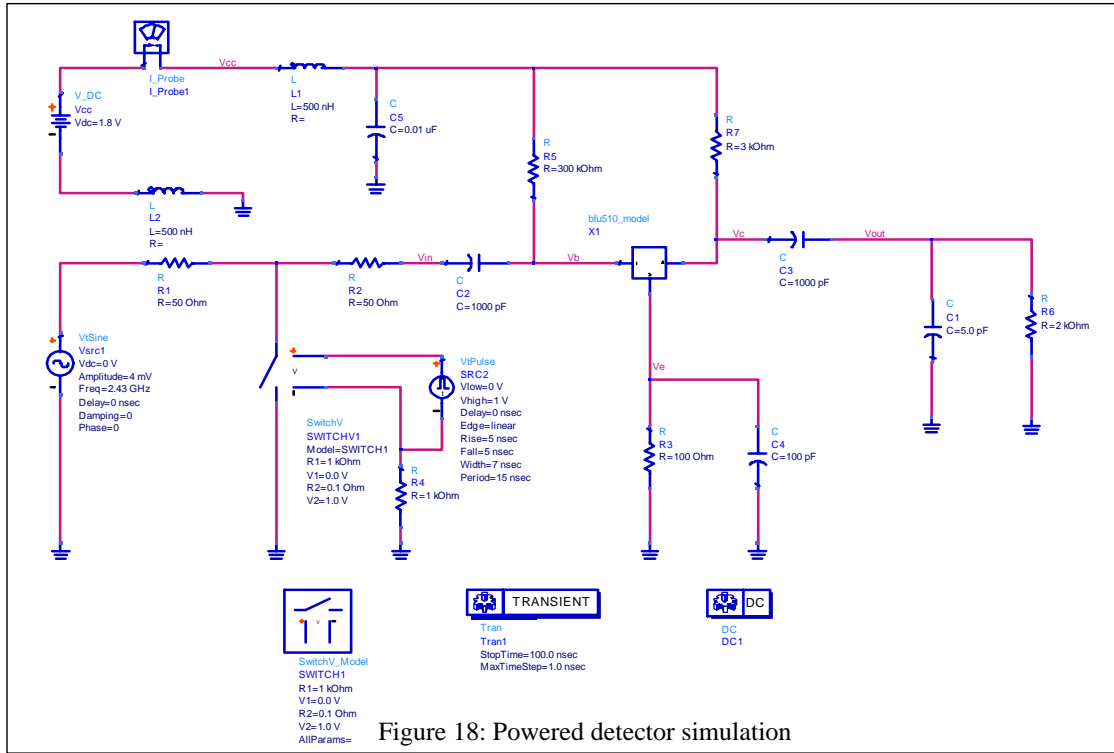


Figure 18: Powered detector simulation

The fifth and sixth approaches shown in the table use different configurations of very low powered amplifiers in addition to powered detectors. The addition of these amplifiers greatly increases the sensitivity of the radio. Both approaches use a low power IF amplifier (2.75v @ 2.1mA continuous, 2.75v @ 10.5uA power-cycled). The IF amplifier was tested as a differential amplifier (figure 19) alone and as a differential amplifier with an additional gain stage. The sixth approach makes use of a very low power (2.75v @ 0.91mA continuous, 2.75v @ 4.5uA power-cycled) baseband amplifier in addition to the IF amplifier. The baseband amplifier (figure 20) has a maximum gain of 66dB with a frequency response of 1.8 to 5MHz. The entire setup is shown in figure 21. The two different approaches should ideally be combined into one amplifier with an automatic gain control circuit to adjust to the different input signal levels. The overall circuit will then have a sensitivity range from -50dBm to +7dBm. All approaches are shown without the addition of a pre-amplifier. The addition of a low powered pre-amplifier will improve input reception by the amount of the gain present in the amplifier, up to a maximum of about 40dB. Thus, the maximum sensitivity attainable using the configurations outlined is about -90dBm, giving a total range with a gain-controlled amplifier of about -90dBm to -33dBm.

The seventh and final approach uses a custom digital correlator board (figure 22) in place of the IF correlator and its related detector. The advantage of this approach is that it gives a digital output whenever the signal is detectable. If the signal is not properly detected, it gives zero output voltage. This approach can be integrated with gain controlled IF amplifiers to provide the same signal sensitivity range as the fifth and sixth approaches. This approach still uses the high-speed SAW

correlators and their related demodulator/ detectors as well as IF amplifiers. The digital correlator board only performs low frequency signal processing and so can operate at relatively low power consumption. It was built as a 16-chip programmable correlator and can easily be made longer. It extends the total code length of the long correlator to 496 chips.

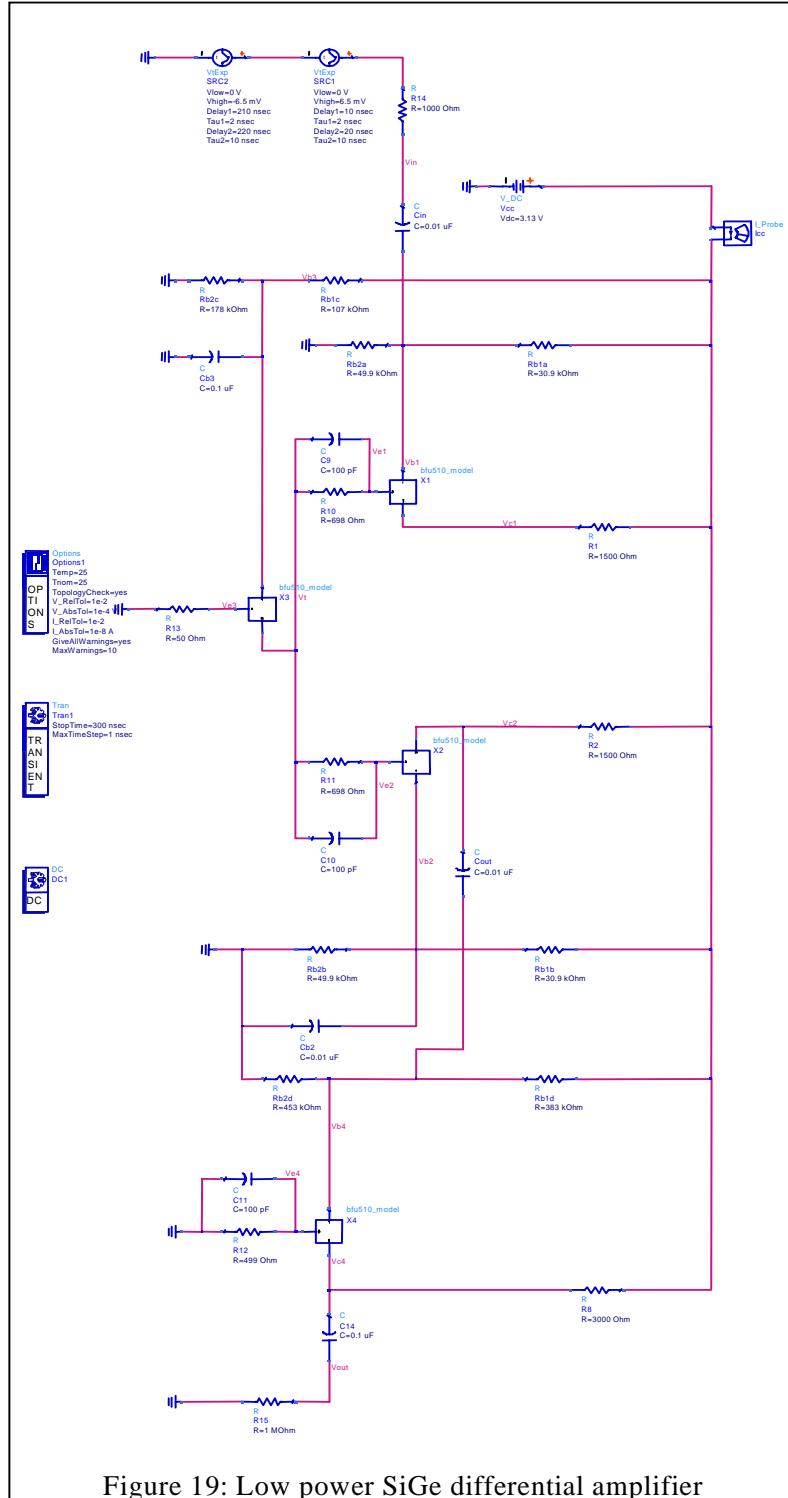


Figure 19: Low power SiGe differential amplifier

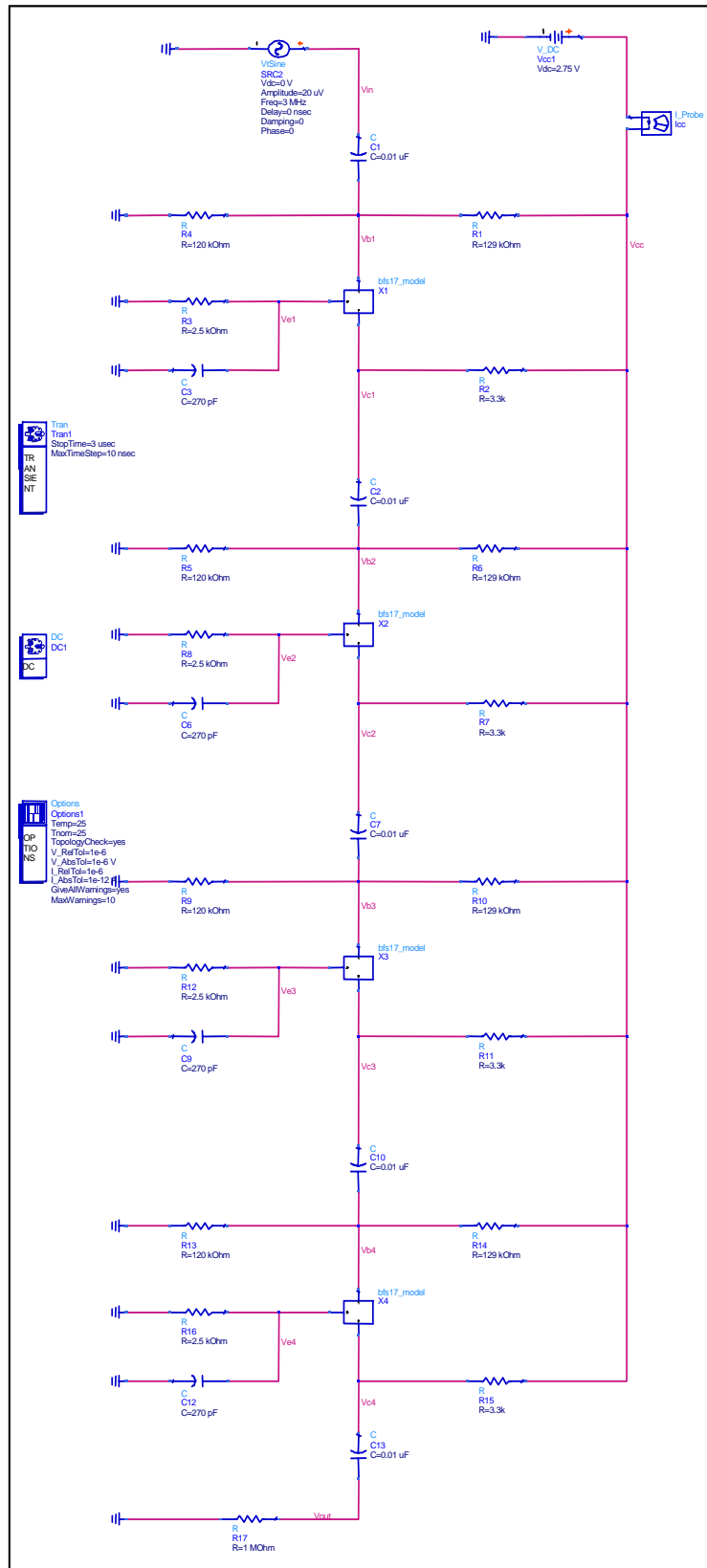


Figure 20: Low power, low frequency baseband amplifier

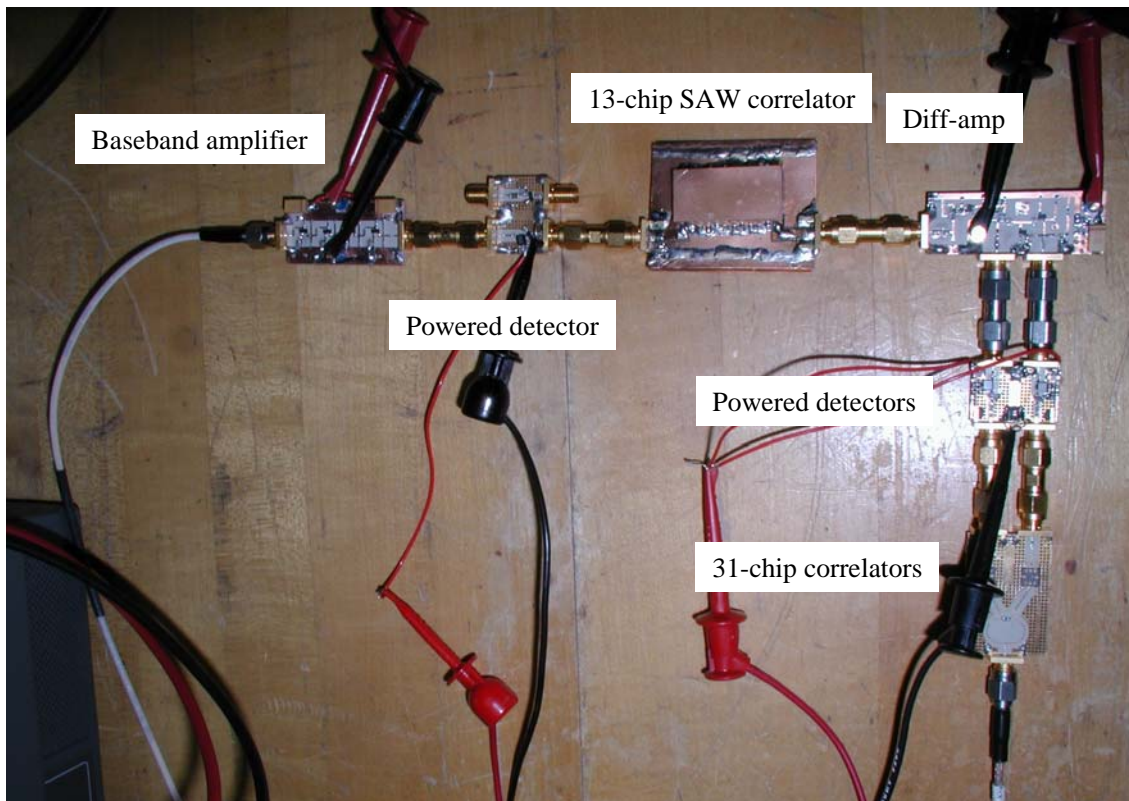


Figure 21: 31-chip correlator, powered detectors, IF diff-amp, 13-chip correlator, and baseband amp.

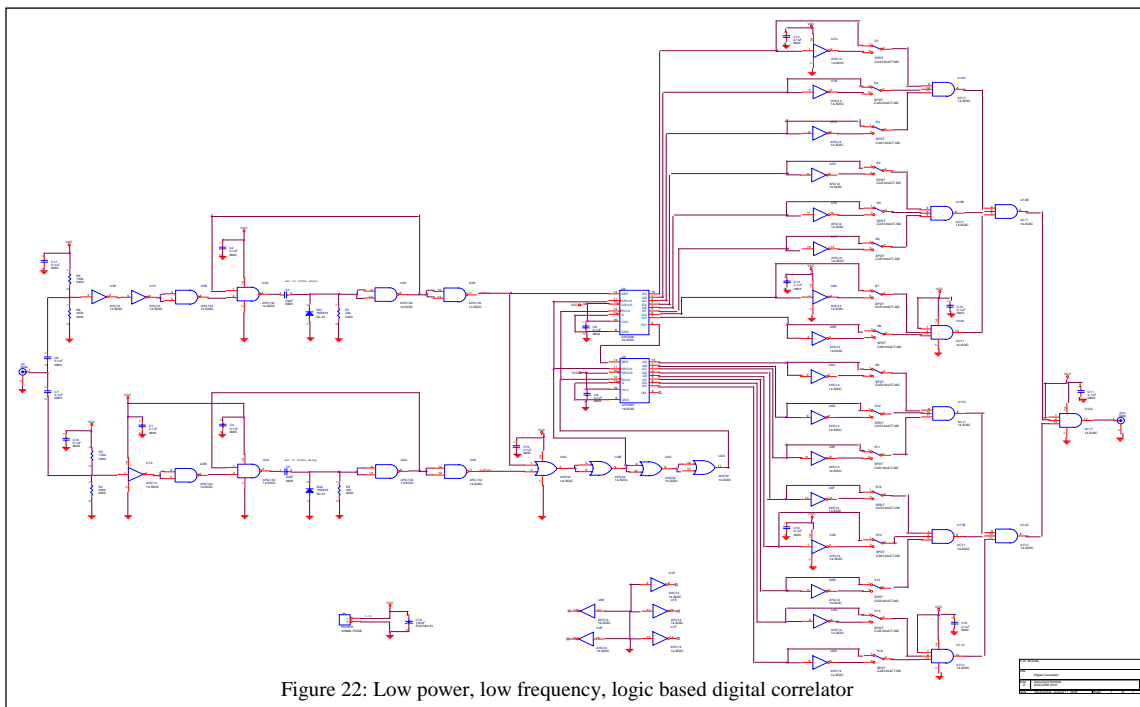


Figure 22: Low power, low frequency, logic based digital correlator

## Conclusions

Zero-power radio receivers suitable for a variety of different applications were devised, built, and tested. The SAW correlators built for the various zero-power radios exhibited very good levels of performance. However, true zero-power radio performance is only adequate in high signal level applications. Improvements to passive demodulator/ detectors are needed to improve the low signal reception capabilities of the zero-power radio. Significant performance improvements in radio performance were obtained by using very low power detectors and amplifiers. The current SAW correlator-based radios suitable for a wide-range of applications are very low powered receivers, possibly lower than any other comparable technology. True zero-power radio receivers based on SAW correlators are very viable but need improved passive detectors to achieve high levels of sensitivity.

## References:

- 1) Ziemer, R.E., and Tranter, W.H., *Principles of Communications*, Houghton Mifflin Co., 1976, pp. 311-317.
- 2) Campbell, Colin K., "Surface Acoustic Wave Devices for Mobile and Wireless Communication," Academic Press, San Diego, 1998, p. 11.
- 3) Lever, K.V., et al, "Analysis of Effect of Fabrication Errors on Performance of Surface-Acoustic-Wave M-sequence Correlators," *Proc. IEE*, Vol. 122, No. 12, Dec. 1975, pp. 1333-1338.
- 4) Biran, A., "Low-Sidelobe SAW Barker 13 Correlator," *IEEE 1985 Ultrasonics Symp.*, pp. 149-152.

## Distribution

8	MS0874	Robert W. Brocato, 1751
5	MS0874	David W. Palmer, 1751
1	MS0874	Glenn D. Omdahl, 1751
1	MS0874	Gregg A. Wouters, 1751
1	MS0874	Matthew A. Montano, 1751
1	MS0874	Emmett J. Gurule, 1751
1	MS0874	Christopher L. Gibson, 1751
1	MS0603	Edwin J. Heller, 1763
1	MS0603	Joel R. Wendt, 1743
1	MS0603	Jonathan D. Blaich, 1763
1	MS0865	Regan W. Stinnett, 1903
1	MS1071	Michael G. Knoll, 1730
1	MS1202	Ann N. Campbell, 5940
2	MS1202	John P. Anthes, 5940
1	MS0574	Robert C. Ghormley, 5945
2	MS1078	Stephen J. Martin, 1707
1	MS0123	LDRD Office, Donna L. Chavez
1	MS0612	Corporate Records, Arlene Lucero
1	MS9018	Central Technical Files, 8945-1
2	MS0899	Technical Library, 9616
1	MS0612	Review and Approval Desk for DOE/OSTI, 9612